

# Model Study on the Pyridine–Dewar Pyridine and Some Related Photoisomerization Reactions

Ming-Der Su<sup>†</sup>

Department of Applied Chemistry, National Chiayi University, Chiayi 60004, Taiwan

Received: August 1, 2006; In Final Form: December 7, 2006

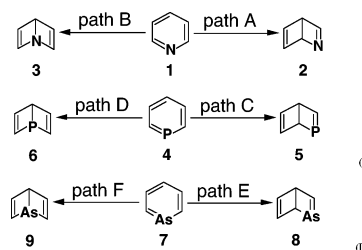
The potential energy surfaces corresponding to the photochemical reactions of pyridine, phosphinine, and arsabenzene have been investigated by employing the CAS(6,6)/6-311G(d,p) and MP2-CAS-(6,6)/6-311++G(3df,3pd)/CAS(6,6)/6-311G(d,p) methods. The thermal (or dark) reactions of these reactant species have also been examined using the same level of theory. The mechanisms of drastic structural change in the excited- and ground-state reactions of pyridine, phosphinine, and arsabenzene and the differences between them are elucidated. The theoretical investigations suggest that conical intersections play a crucial role in their photoisomerization reactions. The results obtained allow a number of predictions to be made.

## Introduction

The photochemistry of heterocyclic aromatic systems is one of the topical fields of research in organic chemistry, biochemistry, and catalytic research.<sup>1</sup> During the past four decades, an enormous amount of experimental work has been aimed at examining the photoisomerization of six-membered heterocycles. Of these, pyridine itself has been the subject of numerous photochemical and spectroscopic investigations.<sup>2,3</sup> In the 1970s, it was reported that irradiation of pyridine (**1**) at 2537 Å in butane at –15 °C yields Dewar pyridine, 2-azabicyclo[2,2,0]hexa-2,5-diene (**2**), which has been characterized and trapped by sodium borohydride<sup>4</sup> and water.<sup>5</sup> In addition, it was also found that Dewar pyridine reverts completely to pyridine within 15 min at room temperature.<sup>4</sup> See Scheme 1.

It is these fascinating photochemical results that inspired this study. Besides the unknown reaction mechanism, several questions still remain unsolved so far. For example, why does irradiation of pyridine not lead to formation of the valence-bonded isomer 2-azabicyclo[2,2,0]hexa-2,5-diene (**3**)? If Dewar pyridine is formed initially on irradiation of pyridine, is it possible to extend this to phosphorus and arsenic heterocyclic analogues? And what are the energies and structures of the critical points, if they exist, and the transition states (TSs) of the photoreactions? To address the above questions, we have undertaken an investigation of the potential energy surfaces of nitrogenarenes, phospharenes, and arsenicarenes.

In the present study, the reaction mechanisms of eqs I, II, and III were investigated by CASSCF calculations in which pyridine (**1**), phosphinine (**4**), and arsabenzene (**7**) were used as model systems, respectively. It will be shown below that the conical intersection (CI) points<sup>6</sup> should play a crucial role in the photoisomerization reactions of these compounds.

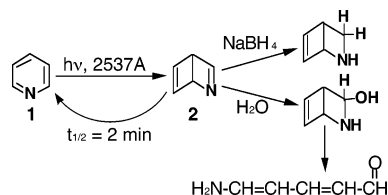


The computational results at the ab initio CASSCF<sup>6,7</sup> level of theory were obtained using the Gaussian 03 software package.<sup>8</sup> In the investigation of the photochemical reaction pathways, the six electrons in six p- $\pi$  orbitals, the CASSCF method was used with the 6-311G(d,p) basis sets for geometry optimization. The optimization of CIs was achieved in the ( $f - 2$ )-dimensional intersection space using the method of Bearpark et al.<sup>7</sup> implemented in the Gaussian 03 program. Minima and TSs were confirmed by the calculations of harmonic vibrational frequencies along the reaction path. Reaction pathways from the TSs were followed by intrinsic reaction coordinate calculations. Because it was reported that the addition of high-exponent d and f inner polarization functions are essential for obtaining reliable energies of second- and third-row species in some cases,<sup>9</sup> we thus used the 6-311++G(3df,3pd) basis sets. To correct the energetics for dynamic electron correlation, single-point calculations were made at the MP2-CAS-(6,6)/6-311++G(3df,3pd) level using CAS(6,6)/6-311G(d,p) geometry (depicted in MP2/CASSCF). Unless otherwise noted, the relative energies given in the text are those determined at the MP2 level.

Let us first consider the photoisomerization of pyridine as indicated in eq I. Two minimum-energy pathways on the singlet excited potential energy surface of pyridine were characterized by optimizing the geometries along the N–C<sub>1</sub> coordinate (path A) and the C<sub>1</sub>–C<sub>2</sub> coordinate (path B), which can lead to products **2** and **3**, respectively. For an understanding of the difference found between the two reaction paths, it is best to start the discussion with the reaction profiles as summarized in Figure 1, which also contains the relative energies of the various

<sup>†</sup> E-mail: midesu@mail.nyu.edu.tw.

## SCHEME 1



points with respect to the energy of the reactant. Some selected geometrical parameters optimized for the stationary points and conical intersections are collected in Figure 2. Cartesian coordinates and energetics calculated for the various points at the CASSCF level are available as Supporting Information.

In the first step the reactant (pyridine) is excited to its excited singlet state by a vertical excitation, as shown in the middle of Figure 1. After the vertical excitation process the molecule is situated on the excited singlet surface but still possesses the  $S_0$ (ground-state) geometry. It was experimentally reported that singlet excitation energies for the low-lying valence  $n \rightarrow \pi^*$  ( $S_1$ ) and  $\pi \rightarrow \pi^*$  ( $S_2$ ) states in pyridine are 4.59 and 4.90 eV, respectively.<sup>2c</sup> According to the previous experimental work,<sup>2,3</sup> the photoexcitation of pyridine with 2537 Å (=4.90 eV in energy) light can lead to the lowest<sup>1</sup> ( $\pi \rightarrow \pi^*$ ) state.<sup>3</sup> Our MP2//CASSCF results suggest that the calculated<sup>1</sup> ( $\pi \rightarrow \pi^*$ ) excited-state energy at the Franck–Condon geometry (FC-N) is 122 kcal/mol (=5.27 eV), which reasonably agrees with the experimental observations.<sup>4,5</sup>

From the point reached by the vertical excitation (FC-N) the molecule relaxes to reach an  $S_2/S_0$  CI where the photoexcited system decays nonradiatively to  $S_0$ . Namely, the photochemically active relaxation path starting from the  $S_2$  ( $\pi \rightarrow \pi^*$ ) excited-state of pyridine leads to the  $S_2/S_0$  CI-A and CI-B, which are shown in the right-hand (path A) and left-hand (path B) side of Figure 1, respectively.<sup>10</sup> From the structures of the  $S_2/$

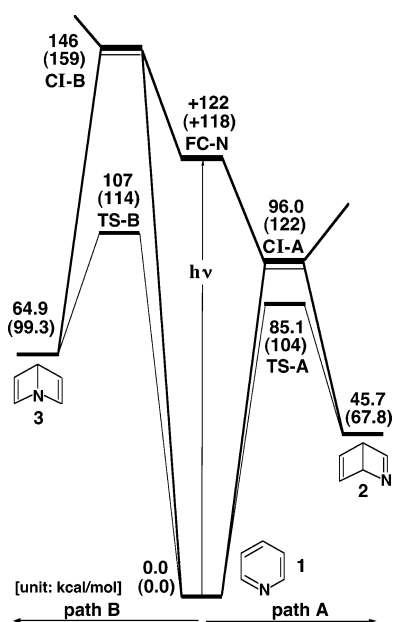


**Figure 1.** Energy profiles for the photochemical rearrangement modes of pyridine (**1**). The abbreviations FC, TS, and CI stand for Franck–Condon, transition state, and conical intersection, respectively. The relative energies were obtained at the MP2-CAS(6,6)/6-311++G(3df,3pd)//CAS(6,6)/6-311G(d,p) and CAS(6,6)/6-311G(d,p) (in parentheses) levels of theory. All energies (in kcal/mol) are given with respect to the reactant  $S_0$ . The CASSCF optimized structures of the stationary points are in Figure 2. For more information see the text.

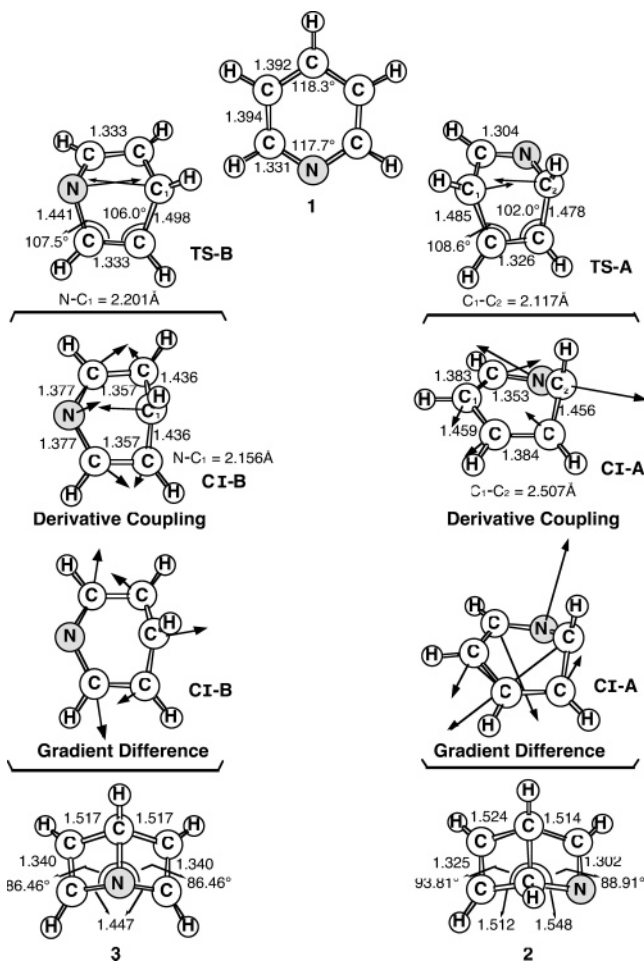


**Figure 2.** CAS(6,6)/6-311G(d,p) geometries (in Å and deg) for the pyridine (**1**), transition states (TS), conical intersection (CI), and isomer products (**2**, **3**). The heavy arrows indicate the main atomic motions in the TS eigenvector. The derivative coupling and gradient difference vectors—those that lift the degeneracy—computed with CASSCF at the conical intersections CI-A and CI-B. The corresponding CASSCF vectors are also shown. For more information see the Supporting Information.

$S_0$  CI-A and CI-B, the nature of the relaxation paths on the  $S_2$  potential surfaces is regarded as C–C and N–C bond formation, respectively. As one can see in Figure 1, our theoretical findings suggest that CI-A is 26 kcal/mol lower in energy than FC-N, whereas CI-B lies 24 kcal/mol above FC-N. On the other hand, the dark reaction on the ground-state potential energy surface is also examined. Although photoexcitation raises pyridine into an excited electronic state, the products of the photochemical process are controlled by the ground-state (thermal) potential surface. The search for TSs on the  $S_0$  surface near the structures of CI-A and CI-B gives TS-A and TS-B for reaction paths A and B, respectively. As shown in Figure 1, the energy of the TS-A connecting **1** and **2** on the  $S_0$  surface lies 12 kcal/mol below the energy of the  $S_2/S_0$  CI-A. Additionally, compound **2** is thermodynamically very unstable by 46 kcal/mol compared with pyridine **1**, but the barrier height between **1** and **2** is quite high (85 kcal/mol from **1**). Similarly, for the dark reaction of path B, compound **3** and its relevant transition structure (TS-B) lie 65 and 107 kcal/mol above pyridine **1**, respectively.

Accordingly, our calculations can provide an explanation of the experimental findings.<sup>4,5</sup> In our interpretation, because our best estimate places CI-A 26 and 50 kcal/mol below FC-N and its competing CI-B, respectively, path A is strongly preferred over path B, and molecule **3** cannot be produced during the

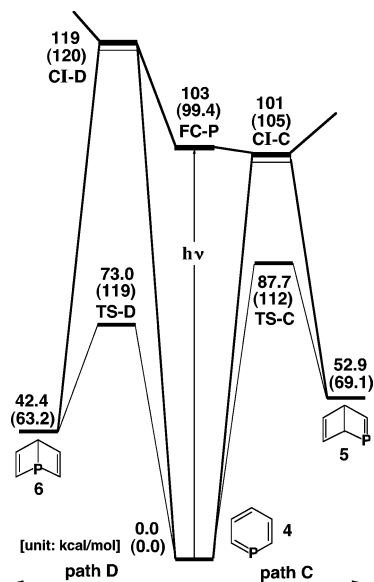


**Figure 3.** Energy profiles for the photochemical rearrangement modes of phosphinine (**4**). The abbreviations FC, TS, and CI stand for Frank–Condon, transition state, and conical intersection, respectively. The relative energies were obtained at the MP2-CAS-(6,6)/6-311++G(3df-3pd)//CAS(6,6)/6-311G(d,p) and CAS(6,6)/6-311G(d,p) (in parentheses) levels of theory. All energies (in kcal/mol) are given with respect to the reactant  $S_0$ . The CASSCF optimized structures of the stationary points are in Figure 4. For more information see the text.

irradiation of pyridine with 2537 Å light. Moreover, path A can lead to either the direct regeneration of the initial ground-state reactant (**1**) or the ultrafast production of a reactant isomer (**2**). Then the new ground-state **2** species can revert to the starting molecule **1** in a thermal process on the ground state as shown in Figure 1. It should be mentioned that the pyridine molecule possesses an excess energy of about 50 kcal/mol arising from the relaxation to the local minimum **2**, which is larger than the energy difference between TS-A and **2** (39 kcal/mol). As a consequence, our model calculations are consistent with the fact that Dewar pyridine **2** can revert to pyridine **1** without any difficulty at room temperature after irradiation. Besides these, due to the energy difference between TS-A and **2** mentioned above, it is likely that **2** should be detected experimentally in photochemical reaction products at low temperature. In fact, this prediction is in accord with one available experimental work.<sup>3a</sup>

Further, the photorearrangement of phosphinine **4** as described in eq II is also examined. Because the computed energy profiles of the pyridine compound can nicely explain the available experimental observations, we are confident that the present models with the method (MP2//CASSCF) employed in this study should provide reliable information for the discussion of the photoisomerization of phosphinine. The reaction profiles computed for eq II of model compound **4** (Figure 3) resemble that of pyridine **1**. Figure 3 is thus arranged as Figure 1, its center indicating the reactant ( $S_0$ ) and FC-P ( $S_0$  geometry), and the reaction profiles of the C–C and P–C bond formation depicted to the right-hand (path C) and the left-hand (path D) sides, respectively.<sup>11</sup> Selected optimized geometrical parameters for the various points can be taken from Figure 4. Cartesian coordinates and energetics calculated for the various points at the CASSCF level are available as Supporting Information.

The computed vertical excitation energy of model compound **4** ( $1(\pi \rightarrow \pi^*)$ ) is 103 kcal/mol, which is lower than that of pyridine (122 kcal/mol). As seen in Figure 3, the MP2//CASSCF results suggest that CI-C is lower than FC-P by 2.0 kcal/mol in

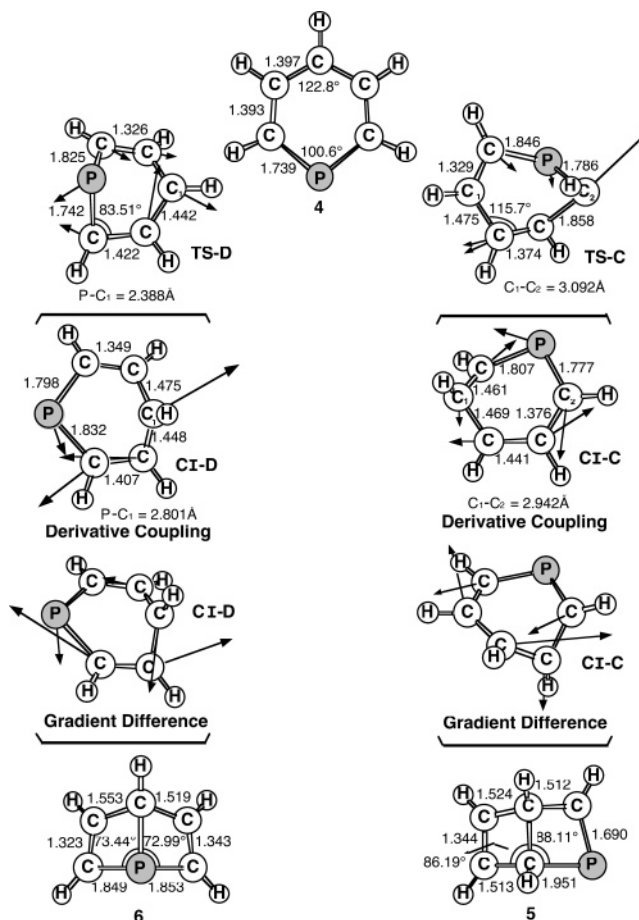


**Figure 4.** CAS(6,6)/6-311G(d,p) geometries (in Å and deg) for the phosphinine (**4**), transition states (TS), conical intersection (CI), and isomer products (**5**, **6**). The heavy arrows indicate the main atomic motions in the TS eigenvector. The derivative coupling and gradient difference vectors—those that lift the degeneracy—computed with CASSCF at the conical intersections CI-C and CI-D. The corresponding CASSCF vectors are also shown. For more information see the Supporting Information.

energy, whereas the competing CI-D is higher than FC-P by 16 kcal/mol in energy. Accordingly, our computations predict that the photochemical rearrangement reaction of path C (**4** → **5**) should be a barrierless process. That is, starting from the FC-P point, phosphinine enters an extremely efficient decay channel, CI-C. After decay at this CI, the Dewar isomer **5** as well as the initial reactant **4** can be reached via a barrierless ground-state relaxation pathway. On the other hand, the formation of a P–C bond (path D) by irradiation of **4** is predicted to be quite difficult, because we could not find a barrierless reaction path from FC-P to the valence-bond isomer **6**. Consequently, our theoretical investigations predict that phosphinine isomer **6** cannot exist during the photoisomerization ( $1(\pi \rightarrow \pi^*)$ ) of phosphinine.

Like the case of pyridine, we also investigated the ground-state (thermal) potential surfaces of **4**, which are given in Figure 3. The search for TSs on the  $S_0$  surface near the structures of  $S_2/S_0$  CI-C and CI-D gives TS-C connecting **4** and **5** and TS-D connecting **4** and **6**, respectively. Our model calculations indicate that the energy of CI-C is higher than that of **4** and **5** by 88 and 35 kcal/mol, respectively, and CI-D lies 73 and 31 kcal/mol above **4** and **6**, respectively. As a result, owing to the high excess energy of about 48 kcal/mol resulting from CI-C to **5**, the barrier (35 kcal/mol) from **5** to TS-C can be easily surmounted. Our computational results also indicated that the barrier height from

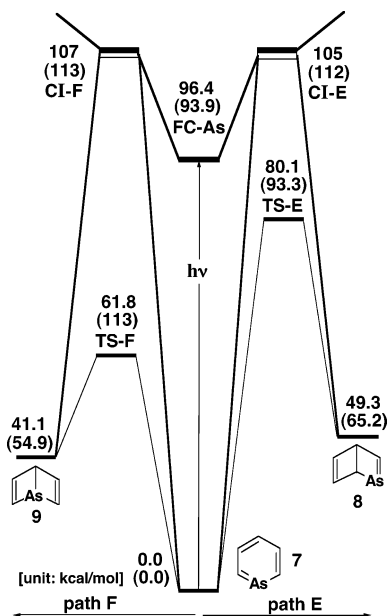
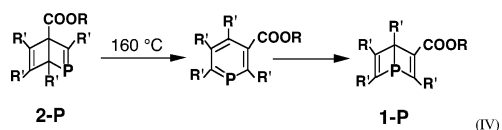


**Figure 5.** Energy profiles for the photochemical rearrangement modes of arsabenzene (**7**). The abbreviations FC, TS, and CI stand for Frank–Condon, transition state, and conical intersection, respectively. The relative energies were obtained at the MP2-CAS-(6,6)/6-311++G(3df-3pd)/CAS(6,6)/6-311G(d,p) and CAS(6,6)/6-311G(d,p) (in parentheses) levels of theory. All energies (in kcal/mol) are given with respect to the reactant  $S_0$ . The CASSCF optimized structures of the stationary points are in Figure 6. For more information see the text.

**4** to TS-C (88 kcal/mol) is higher than that from **4** to TS-D (73 kcal/mol). All these data strongly suggest that, once Dewar phosphinine **5** is formed, it should easily convert to another isomer, **6**. The supporting evidence comes from the fact that the rearrangement of the 2-P Dewar molecule into the corresponding 1-P isomer via the 2-coordinate phosphinine is observed around 160 °C. See eq IV.<sup>12</sup>



Finally, we studied the photorearrangement of arsabenzene (**7**) as given in eq III. Two reaction pathways along the As–C<sub>1</sub> coordinate (path E) and the C<sub>1</sub>–C<sub>2</sub> coordinate (path F) have been examined at the same level of theory. Energy values for the various stationary points and CIs at singlet ground and excited states are given in Figure 5, and selected geometrical parameters optimized at these crucial points can be taken from Figure 6.<sup>13</sup> The geometry optimization starting from  $S_2(S_0$  geom) leads to CIs (i.e., CI-E and CI-F) about 8.6 and 11 kcal/mol higher in energy, respectively. That is, for the arsabenzene **7** model system, we calculate much higher CI energies than those in  $S_2(S_0$  geom). We therefore expect that the singlet excited energy of **7** (96 kcal/mol) is insufficient to yield products **8** and **9** through radiationless decay (i.e., the CI channel). Accordingly, no photoreaction should be observed in the arsabenzene **7** system. Namely, our theoretical findings suggest that the photorearrangement products of arsabenzene **7** are not produced from the  $^1\pi \rightarrow ^1\pi^*$  excitation reactions followed by the CI channels but possibly exist if these compounds (**8** and **9**) are produced through other reaction paths.

Furthermore, one may wonder why there exists the increasing energy of the CI-A, CI-C, and CI-E (or CI-B, CI-D, and CI-F),

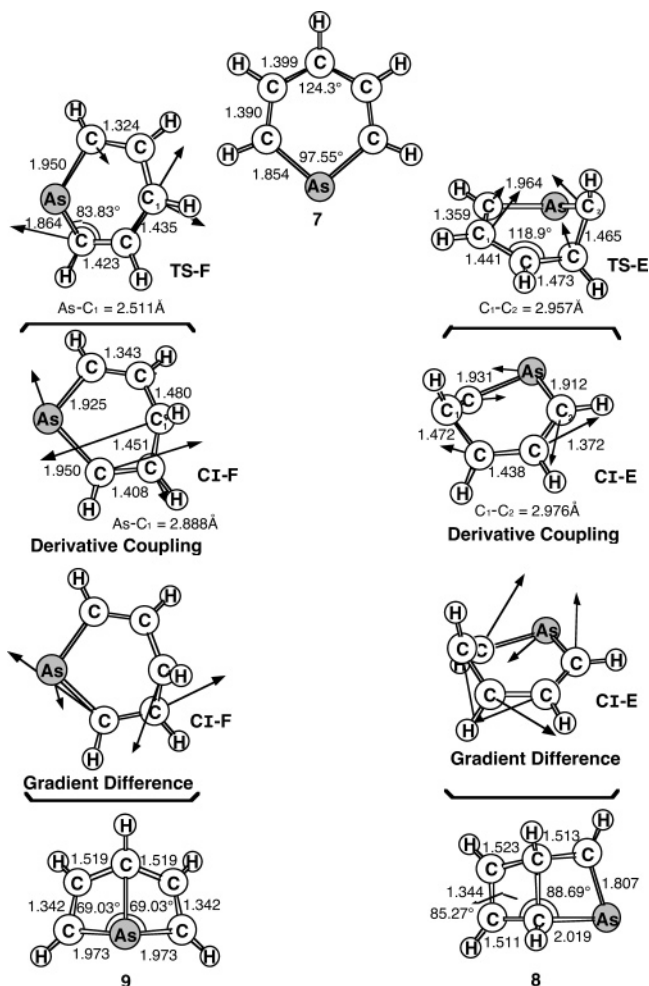


**Figure 6.** CAS(6,6)/6-311G(d,p) geometries (in Å and deg) for the arsabenzene (**7**), transition states (TS), conical intersection (CI), and isomer products (**8**, **9**). The heavy arrows indicate the main atomic motions in the TS eigenvector. The derivative coupling and gradient difference vectors—those that lift the degeneracy—computed with CASSCF at the conical intersections CI-E and CI-F. The corresponding CASSCF vectors are also shown. For more information see the Supporting Information.

when going down in the periodic table. In fact, this phenomenon is quite similar to the pyramidal inversion of an amine. It was experimentally reported that the barrier to nitrogen inversion is about 6.0 kcal/mol, which is only twice as large as the barrier to rotation about a C–C single bond.<sup>14</sup> As a result, pyramidal inversion is so rapid at room temperature that the two enantiomeric pyramid forms cannot normally be isolated. However, the difficulty for such pyramidal inversion show a monotonic increase down the group from N to Bi.<sup>15</sup> That is, the barrier to pnicogen inversion increases with decreasing electronegativity. The reason for this may be the atomic weight of the pnicogen. From this, one may easily anticipate that the lighter the atomic number of pnicogen, the easier the photorearrangement of pyridine to Dewar pyridine.

Also, one may ask whether it is possible for the participation of the spin–orbit coupling and triplet states in arsabenzene. However, according to the heavy atom effect,<sup>16</sup> it is suggested that the photorearrangement of arsabenzene should be via a singlet path, rather than a triplet route, and the spin–orbit coupling effect can be neglected. Consequently, it is believed that a singlet process due to the effect of heavy atoms should play a decisive role in the photoisomerization of arsabenzene.

In short, the nice agreement between our results and the experimentally observed findings in the pyridine system gives us confidence to predict that the Dewar phosphinine **5** can be easily produced by irradiation of phosphinine **4**, whereas no photorearrangement ( $^1(\pi \rightarrow \pi^*)$ ) can be observed in the arsbenzene **7** system.

We eagerly await experimental results to confirm our predictions.

**Acknowledgment.** I am grateful to the National Center for High-Performance Computing of Taiwan for generous amounts of computing time, and the National Science Council of Taiwan for the financial support. I also thank Professor Michael A. Robb, Dr. Michael J. Bearpark (University of London, U.K.), Professor Massimo Olivucci (Universita degli Studi di Siena, Italy), and Professor Fernando Bernardi (University of Bologna, Italy) for their encouragement and support during my stay in London. Special thanks are also due to Reviewer 66 for helpful suggestions and comments.

**Supporting Information Available:** CASSCF optimized geometries and MP2-CAS and CASSCF energies. This material is available free of charge via the Internet at <http://pubs.acs.org>.

## References and Notes

- (1) For reviews, see: (a) Nastasi, M.; Streith, J. In *Rearrangements in Ground and Excited States*; De Mayo, P., Ed.; Academic Press: New York, 1980; Vol. 3, p 445. (b) Padwa, A. In *Rearrangements in Ground and Excited States*; De Mayo, P., Ed.; Academic Press: New York, 1980; Vol. 3, p 501. (c) Lablache-Combiere, A. In *Photochemistry of Heterocyclic Compounds*; Buchardt, O., Ed.; Wiley: New York, 1976; Chapter 3. (d) Lablache-Combiere, A. In *Photochemistry of Heterocyclic Compounds*; Buchardt, O., Ed.; Wiley: New York, 1976; Chapter 4. (e) Whitten, D. G. In *Photochemistry of Heterocyclic Compounds*; Buchardt, O., Ed.; Wiley: New York, 1976; Chapter 8.
- (2) For instance, see: (a) McGlynn, S. P.; Azumi, T.; Kinoshita, M. *Molecular Spectroscopy of the Triplet State*; Prentice Hall: London, 1969. (b) Ross, I. G. In *Photochemistry of Heterocyclic Compounds*; Buchardt, O., Ed.; Wiley: New York, 1976; Chapter 1. (c) Nagaoka, S.; Nagashima, U. *J. Chem. Phys.* **1990**, *94*, 4467. (d) Nooijen, M.; Bartlett, R. J. *J. Chem. Phys.* **1997**, *106*, 6441. (e) Chachisvilis, M.; Zewail, A. H. *J. Chem. Phys. A* **1999**, *103*, 7408 and references therein.
- (3) (a) Pavlik, J. W.; Kebede, N.; Thompson, M.; Day, A. C.; Barltrop, J. A. *J. Am. Chem. Soc.* **1999**, *121*, 5666. (b) Cao, Z.; Zhang, Q.; Peyerimhoff, S. D. *Chem. Eur. J.* **2001**, *7*, 1927.
- (4) (a) Wilzbach, K. E.; Rausch, D. J. *J. Am. Chem. Soc.* **1970**, *92*, 2178. (b) Joussot-Dubien, J.; Houdard-Peyrere, J. *Tetrahedron Lett.* **1967**, 4389. (c) Joussot-Dubien, J.; Houdard-Peyrere, J. *Bull. Soc. Chim. Fr.* **1967**, 2619.
- (5) A recent study of femtosecond dynamics as well as theoretical calculations of pyridine by Zewail and Chachisvilis explored the photochemical dynamics of the  $S_2(\pi \rightarrow \pi^*)$  excited state leading to the formation of the azaprefulvene isomer. Also, they found that the reaction path on the  $S_2(\pi \rightarrow \pi^*)$  potential energy surface was the lowest path for the formation of the azaprefulvene isomer at the CASSCF level. See ref 2e. We are therefore confident that a pyridine species with biradical character, originating from the excited state  $S_2(\pi \rightarrow \pi^*)$ , should be a precursor in the interversion of the pyridine.
- (6) For recently excellent reviews, see: (a) Bernardi, F.; Olivucci, M.; Robb, M. A. *Isr. J. Chem.* **1993**, 265. (b) Klessinger, M. *Angew. Chem. Int. Ed. Engl.* **1995**, *34*, 549. (c) Bernardi, F.; Olivucci, M.; Robb, M. A. *Chem. Soc. Rev.* **1996**, 321. (d) Bernardi, F.; Olivucci, M.; Robb, M. A. *J. Photochem. Photobiol. A: Chem.* **1997**, *105*, 365. (e) Klessinger, M. *Pure Appl. Chem.* **1997**, *69*, 773.
- (7) (a) Bearpark, M. J.; Robb, M. A.; Schlegel, H. B. *Chem. Phys. Lett.* **1994**, *223*, 269. (b) For more details, see ref. (6c) and references therein.
- (8) Frisch, M. J.; Trucks, G. W.; Schlegel, H. B.; Scuseria, G. E.; Robb, M. A.; Cheeseman, J. R.; Zakrzewski, V. G.; Montgomery, J. A., Jr.; Stratmann, R. E.; Burant, J. C.; Dapprich, S.; Millam, J. M.; Daniels, A. D.; Kudin, K. N.; Strain, M. C.; Farkas, O.; Tomasi, J.; Barone, V.; Cossi, M.; Cammi, R.; Mennucci, B.; Pomelli, C.; Adamo, C.; Clifford, S.; Ochterski, J.; Petersson, G. A.; Ayala, P. Y.; Cui, Q.; Morokuma, K.; Malick, D. K.; Rabuck, A. D.; Raghavachari, K.; Foresman, J. B.; Cioslowski, J.; Ortiz, J. V.; Baboul, A. G.; Stefanov, B. B.; Liu, Liashenko, G.; Piskorz, A.; Komaromi, P.; I.; Gomperts, R.; Martin, R. L.; Fox, D. J.; Keith, T.; Al-Laham, M. A.; Peng, C. Y.; Nanayakkara, A.; Gonzalez, C.; Challacombe, M.; Gill, P. M. W.; Johnson, B.; Chen, W.; Wong, M. W.; Andres, J. L.; Gonzalez, C.; Head-Gordon, M.; Replogle, E. S.; Pople, J. A. *Gaussian, Inc.: Pittsburgh, PA*, 2003.
- (9) (a) Bauschlicher, C. W., Jr.; Partridge, H. *Chem. Phys. Lett.* **1995**, *240*, 533. (b) Martin, J. M. L. *J. Chem. Phys.* **1998**, *108*, 2791.
- (10) According to the results outlined in Figure 2, funneling through  $S_2/S_0$  CI (i.e., CI-A and CI-B) leads to two different reaction paths on the ground-state surface, via either the derivative coupling vector or the gradient difference vector. For instance, the gradient difference vector for CI-A corresponds to an antisymmetric bending motion, which may lead to a vibrationally hot species at the  $S_0$  configuration. On the other hand, its derivative coupling vector corresponds to the intramolecular formation of a Dewar pyridine, **2**. Besides these, again, the derivative coupling vector for CI-B can lead to the isomer **3**, whereas its gradient difference vector may result in a vibrationally hot species at the  $S_0$  configuration.
- (11) According to the results shown in Figure 4, funneling through  $S_2/S_0$  CI (i.e., CI-C and CI-D) leads to two different reaction paths on the ground-state surface, via either the derivative coupling vector or the gradient difference vector. For example, the gradient difference vector for CI-C can lead to a vibrationally hot species at the  $S_0$  configuration, whereas its derivative coupling vector can result in an isomer, **5**. Likewise, the same situation can also be found in the left-hand side of Figure 4; that is, the gradient difference vector for CI-D can result in a vibrationally hot species at the  $S_0$  configuration, and its derivative coupling vector can lead to an isomer, **6**.
- (12) Blatter, K.; Rosch, W.; Vogelbacher, U.-J.; Fink, J.; Regitz, M. *Angew. Chem., Int. Ed. Engl.* **1987**, *26*, 85.
- (13) Again, according to the results displayed in Figure 6, funneling through  $S_2/S_0$  CI (i.e., CI-E and CI-F) leads to two different reaction paths on the ground-state surface, via either the derivative coupling vector or the gradient difference vector. The derivative coupling vector for CI-E can lead to a vibrationally hot species at the  $S_0$  configuration. However, its gradient difference vector can result in a Dewar isomer, **8**. Similarly, the gradient difference vector for CI-F can lead to vibrationally hot species at the  $S_0$  configuration, and its derivative coupling vector can lead to an isomer, **9**.
- (14) Mcmurry, J. In *Organic Chemistry*, 6th ed.; Thomson: New York, 2004; pp 895–896.
- (15) Su, M.-D. Unpublished results.
- (16) For more details, see: Su, M.-D. *J. Phys. Chem.* **1996**, *100*, 4339.